Lack of Ultrametricity in the Low Temperature phase of 3D Ising Spin Glasses

Guy Hed

Department of Materials and Interfaces,

Weizmann Institute of Science, Rehovot 76100, Israel

A. P. Young

Department of Physics, University of California, Santa Cruz, CA 95064

Eytan Domany

Department of Physics of Complex Systems,

Weizmann Institute of Science, Rehovot 76100, Israel

Abstract

We study the low-temperature spin-glass phases of the Sherrington-Kirkpatrick (SK) model and of the 3-dimensional short range Ising spin glass (3dISG). By using clustering to focus on the relevant parts of phase space and reduce finite size effects, we found that for the SK model ultrametricity becomes clearer as the system's size increases, while for the short-range case our results indicate the opposite, i.e. lack of ultrametricity. Another method, which does not rely on clustering, indicates that the mean field solution works for the SK model but does not apply in detail to the 3dISG, for which stochastic stability is also violated.

Spin glasses constitute an example of a fascinating family of physical systems, in which the combination of disorder and frustration produces a multitude of low-lying states, unrelated by symmetry. A major breakthrough came with Parisi's mean-field solution [1] of the infinite-range Sherrington-Kirkpatrick (SK) model [2]; a complex low-temperature phase with rich structure was revealed. One of the central open questions of the field is whether the qualitative structure of the mean-field solution is valid also for the experimentally relevant 3-dimensional short-range Ising Spin Glasses (3dISG). Both systems are described by the N-spin Hamiltonian

$$H(\vec{s}) = -\sum_{\langle i,j \rangle} J_{ij} s_i s_j \ , \tag{1}$$

where $s_i = \pm 1$. In the SK model the sum in Eq. (1) runs over all pairs of spins, while in the 3dISG the sum is over nearest neighbor sites of a cubic lattice. The interactions J_{ij} are taken from a Gaussian distribution with mean zero and variance $1/(N-1)$ in the SK model, while the variance is 1 for the 3dISG.

To test the validity of the mean field solution, it is natural to consider first the most widely calculated observable in ISG; the distribution $P(q)$ of the overlaps q, defined for two states $\vec{s}^{\mu}$ and $\vec{s}^{\nu}$ as $q_{\mu\nu} = N^{-1} \sum_{i=1}^{N} s_i^{\mu} s_i^{\nu}$. For each realization of the randomly selected J_{ij} one calculates the probability distribution $P_J(q)$ (at equilibrium at some temperature); $P(q) = [P_J(q)]_{\rm av}$ is the average over the different realizations $\{J\}$ of the disorder. Indeed, $P(q)$ was measured by Monte-Carlo simulations [3] and in other ways [4, 5] and non-trivial overlap distributions were found for both the SK and 3dISG. However, there were clear indications that the nature of the low T phases of the two models were different [6, 7]. In particular, evidence was presented [7] for lack of ultrametricity in 3dISG.

Ultrametricity (UM) of the state space [8] is one of the main characteristics of the low T phase of the mean-field solution and the SK model. Consider an equilibrium ensemble of microstates at $T < T_c$, and pick three, ρ, μ and ν at random (see, however, point (a) below). These indices represent the states $\vec{s}^{\rho}$, $\vec{s}^{\mu}$ and $\vec{s}^{\nu}$. Order them so that $q_{\mu\nu} \geq q_{\nu\rho} \geq q_{\mu\rho}$; ultrametricity means that in the thermodynamic limit we get $q_{\nu\rho} = q_{\mu\rho}$ with probability 1. In terms of the distances $d_{\mu\nu} = (1 - q_{\mu\nu})/2$ the condition of UM becomes $d_{\nu\rho} = d_{\mu\rho} \geq d_{\mu\nu}$.

Even though claims were made for the emergence of UM for large 3D systems [9], these were not conclusive. Since demonstrating lack of ultrametricity suffices to prove that the mean-field solution does not apply for the 3dISG, the evidence presented in [7] prompted

Ciliberti and Marinari (CM) [10] to use similar methods at the same system sizes as used by [7], to search for ultrametricity in the SK model, which has an ultrametric low-T phase. CM did not see UM in the SK model and claimed that the system sizes used were too small to allow observation of ultrametricity. CM argued further that failure to see UM where it holds indicates that similar failure reported [7] for the 3dISG does not provide evidence for its absence.

In order to settle this issue we performed extensive simulations of the SK model for a somewhat larger range of sizes than in CM, and carried out a careful analysis of the results. We also applied the same method of analysis to our earlier [7] results for the 3dISG model. As opposed to CM, we do find clear evidence for UM in the SK model; it's signature becomes more pronounced as the system size increases. On the other hand, for the 3dISG we find the opposite; with increasing system size the results become less consistent with UM. We will explain in detail elsewhere [11] the reasons for the differences between our results and those of CM. Here we note that in order to observe UM one has to avoid three main pitfalls:

(a) If time reversal symmetry is unbroken (zero field), phase space structure consists of two spin-flip related pure-state hierarchies (see Fig. 1). UM can be observed only if all three states of each sampled triplet belong to the same side [10, 12].

(b) Do not work too close to T_c otherwise finite size effects mask the signal.

(c) At low T, most of the microstates belong to the same pure state [8]. With increasing N the overlaps inside a pure state converge to $q_{\rm EA}$ and most $\{\rho, \mu, \nu\}$ triangles become equilateral, conveying no information on UM.

To avoid pitfalls (a) and (c) we map out the upper levels of the pure state hierarchy by clustering [7, 13] (see Fig 1). To avoid (a), we consider only triplets of states from (say) the left tree and to avoid (c) we pick the three states from different pure states of this tree.

Monte Carlo simulations: SK systems were simulated at sizes $N = 32, 128, 256, 1024$. To speed up equilibration we used parallel temperingwith 21 temperatures ranging from 2.0 down to 0.2. Tests for equilibration were carried out as in Ref. 6. Details of the simulations on the 3dISG are given in Ref. 7. For each size we generated 500 different realizations $\{J\}$ of the disorder (except for $N = 8^3$ - only 335 realizations). For each $\{J\}$ we generated 500 microstates, sampled according the Boltzmann distribution at $T = 0.2$. Each sample of

states was enhanced to 1000 by adding to these 500 microstates their spin-flip mirror images. The result is two spin-flip related unbiased samples - one from each tree. The microstates appear in the random order generated by the Monte Carlo procedure.

Identification of pure states by clustering: The 1000 microstates, obtained for a realization of the disorder $\{J\}$, are assigned to groups with a relative tree-like structure [7] by clustering. Here [14] we used the well known *average linkage* agglomerative clustering algorithm [15]. Initially each of the $M = 1000$ points (microstates) is a cluster; at every clustering step those two clusters α, β that are closest are merged to form a new cluster γ; the process stops after $M - 1$ steps when all the points belong to one cluster. The distance $d_{\alpha,\beta}$ between clusters is defined as the average distance between points of α and β. After every merging operation we record for the new cluster $\gamma = \alpha \cup \beta$ the score $s_\gamma = d_{\alpha,\beta}$, and for each of the merged clusters a quality measure $v_\alpha = s_\gamma / s_\alpha$. If v_α is high, the distances between states within α are significantly smaller then the distances of these states from states outside α, and cluster α is "real", i.e. not an artifact of the agglomerative procedure.

Fig. 1 presents the tree of clusters (dendrogram) obtained when the procedure outlined above was applied to the equilibrium ensemble of 1000 microstates, obtained at $T = 0.2$ for a particular realization $\{J\}$ of the SK model with $N = 1024$ spins. The clusters at the higher levels of the hierarchy have high v_α values, suggesting that the partitions they form indeed exist in the underlying distribution from which the states were taken. That is, they map the microstates in our sample to the pure states from which they were taken.

At the highest level, the dendrogram splits into two identical trees, which are the two spin-flip related pure state trees. We consider the states that belong to one (the left). For all $\{J\}$ we call the two top level state clusters by $\mathcal{C}_1$ and $\mathcal{C}_2$ with the convention $|\mathcal{C}_1| \geq |\mathcal{C}_2|$. The two subclusters of $\mathcal{C}_1$ are denoted by $\mathcal{C}_{1a}$ and $\mathcal{C}_{1b}$. The triplets of microstates for which we test UM are selected as follows: $\mu \in \mathcal{C}_{1a}$, $\nu \in \mathcal{C}_{1b}$ and $\rho \in \mathcal{C}_2$. If state space is ultrametric and these clusters correspond to the underlying pure states, we expect $d_{\mu\rho} = d_{\nu\rho} \geq d_{\mu\nu}$.

Direct Measurement of Ultrametricity: For each triplet of states μ, ν and ρ selected as described above, we define an index [7]

$$K_{\mu\nu\rho} = \frac{|d_{\mu\rho} - d_{\nu\rho}|}{d_{\mu\nu}} \ . \tag{2}$$

Note that $0 \leq K_{\mu\nu\rho} \leq 1$ due to the triangle inequality.

For a given realization $\{J\}$ we identify $\mathcal{C}_{1a}$, $\mathcal{C}_{1b}$, and $\mathcal{C}_2$, and measure $K_{\mu\nu\rho}$ over all the

corresponding state triplets. We discard triplets with $K = 1$ since these correspond to colinear "triangles" – they are the result of a finite size effect, and their weight $P(K = 1)$ decreases rapidly with increasing system size, as seen in Table I. We calculate the distribution $P_J(K) = P_J(K_{\rho\mu\nu} = K|K_{\rho\mu\nu} < 1)$, and its mean K_J. We then average over the realizations $\{J\}$ to get $\overline{K} = [K_J]_{\rm av}$ and $P(K) = [P_J(K)]_{\rm av}$. If state space is UM in the thermodynamic limit, we expect $\overline{K} \to 0$ and $P(K) \to \delta(K)$ as $N \to \infty$.

We present in Fig. 2 the distributions $P(K)$ obtained for a sequence of sizes N for the SK and 3dISG models. For the SK model the peak of $P(K)$ is at $K = 0$ and it's width decreases as N increases, as expected if $P(K)$ is to approach $\delta(K)$. The behavior is markedly different for the 3dISG: the width of the distribution remains constant and its peak is at $K \simeq 0.8$. For the SK model the values of $\overline{K}$, presented in Table I, are smaller, decrease faster and approach zero as N increases, whereas for the 3dISG $\overline{K}$ seems to go to a non-vanishing limiting value. For both systems the lowest size is useless for estimating the trend with increasing N.

We present also results obtained for the SK model by a "naive" calculation, that neglects to ensure that all members of a triplet of states are drawn from the same side of the dendrogram; such oversight indeed renders UM unobservable, as also noted by [10, 12].

Another test of UM is the following: if the state space is ultrametric, then the distance between states $\mu \in \mathcal{C}_1$ and $\nu \in \mathcal{C}_2$ depends only on the identity of their closest common ancestor on the tree of pure states, which is $\mathcal{C}_1 \cup \mathcal{C}_2$. Thus, for each realization, the submatrix $q_{\mathcal{C}_1\mathcal{C}_2}$ should be uniform (e.g. the rectangle in the distance matrix of Fig. 1, that connects states from C_1 and C_2, should be uniformly shaded).

We have calculated the standard deviation $s_{\mathcal{C}_1\mathcal{C}_2}$ and the average $m_{\mathcal{C}_1\mathcal{C}_2}$of the elements of $q_{\mathcal{C}_1\mathcal{C}_2}$ for each realization $\{J\}$. For a given average m the standard deviation is bounded by $\sqrt{m(1-m)}$ - the standard deviation of a Bernoulli distribution. We define a normalized standard deviation $S_{\mathcal{C}_1\mathcal{C}_2} = s_{\mathcal{C}_1\mathcal{C}_2}/\sqrt{m_{\mathcal{C}_1\mathcal{C}_2}(1-m_{\mathcal{C}_1\mathcal{C}_2})}$. We average over the realizations to get $[s_{\mathcal{C}_1\mathcal{C}_2}]_{\rm av}$ and $[S_{\mathcal{C}_1\mathcal{C}_2}]_{\rm av}$. The results are given in Table II. For the SK model both $[s_{\mathcal{C}_1\mathcal{C}_2}]_{\rm av}$ and $[S_{\mathcal{C}_1\mathcal{C}_2}]_{\rm av}$ decrease rapidly as N increases, indicating again that UM is approached, while for the 3dISG the values of $[s_{\mathcal{C}_1\mathcal{C}_2}]_{\rm av}$ and $[S_{\mathcal{C}_1\mathcal{C}_2}]_{\rm av}$ seem to asymptote to 0.04 and 0.13 respectively.

To test the validity of the mean field solution without using clustering methods, we focused on one of several results for multi overlap distributions. Mézard et al. [8] showed that the

distributions $P_J(q)$ of ISG satisfy the relation

$$[P_J(q_1)P_J(q_2)]_{\rm av} = \frac{2}{3}P(q_1)P(q_2) + \frac{1}{3}P(q_1)\delta(q_1 - q_2)\ . \tag{3}$$

which, just like UM, is a consequence of Parisi's mean field solution. Eq. (3) has been derived for the SK model without replicas by Guerra [16] and, more generally, is a consequence of "stochastic stability" [17, 18]. In order to test the validity of Eq. (3) we define

$$\rho(q_1, q_2) = \frac{3[P_J(q_1)P_J(q_2)]_{\rm av} - 2P(q_1)P(q_2)}{P(q_1)}\ . \tag{4}$$

We study $\rho(\Delta q)$ - the average of ρ over overlap pairs $\{q_1, q_2\}$ with $|q_1 - q_2| = \Delta q$. As $N \to \infty$ we expect ρ to have a δ-peak at $\Delta q = 0$ [19]. In general, this peak can have a small weight and ρ may have a continuous part, while in the mean field solution $\rho(\Delta q)$ converges to $\delta(\Delta q)$.

Fig. 3 presents $\rho(\Delta q)$. For the SK model ρ approaches $\delta(\Delta q)$ with increasing N, while for the 3dISG the height of the peak at 0 decreases and seems to converge to a finite value, and the width remains constant. For this case we conclude that ρ is the sum of a $\delta(\Delta q)$-peak, and a continuous term; the rise of the first with N is masked by the decrease of the second.

We also examined the equality of the second moment of Eq. (3): $[\langle q^2\rangle^2]_{\rm av} = \frac{2}{3}[\langle q^2\rangle]_{\rm av}^{\ 2} + \frac{1}{3}[\langle q^4\rangle]_{\rm av}$, which has been investigated numerically in other work [20]. We find that the ratio of the two sides is one for both SK and 3dISG of all sizes within an error smaller than 0.03, in agreement with Ref. 20. However, moments may be insensitive to deviations from Eq. (3) because $\rho \approx 0$ when $|q_1 - q_2| > 0.2$.

Top conclude, we have presented strong evidence for the lack of UM in the low T phase of the 3-dimensional short range Ising spin glass. We conclude that our methods *are* able to detect UM, *where it exists*, at the system sizes studied. Our findings indicate that *the structure of the low-temperature phase of spin glasses that emerges from the mean-field solution is not valid for the 3-dimensional short range Ising spin glass.*

We thank E. Marinari and I. Kanter for helpful correspondence and discussions and particularly, G. Parisi for generously sharing his insights and correcting inaccuracies of our preprint. This work was supported by grants from the Minerva Foundation, the Germany-Israel Science Foundation and the European Community's Human Potential Programme under contract HPRN-CT-2002-00319, STIPCO. The work of APY was supported by NSF grants DMR 0086287 and 0337049.

[1] G. Parisi, M. Mézard, and M. A. Virasoro, *Spin glass theory and beyond* (World Scientific, Singapore, 1987).

[2] D. Sherrington and S. Kirkpatrick, Phys. Rev. Lett. **35**, 1792 (1975).

[3] E. Marinari, G. Parisi, and J. J. Ruiz-Lorenzo, Phys. Rev. B **58**, 14852 (1998).

[4] F. Krzakala and O. C. Martin, Phys. Rev. Lett. **85**, 3013 (2000).

[5] M. Palassini and A. P. Young, Phys. Rev. Lett. **85**, 3017 (2000).

[6] H. G. Katzgraber, M. Palassini, and A. P. Young, Phys. Rev. B **63**, 184422 (2001).

[7] E. Domany, G. Hed, M. Palassini, and A. P. Young, Phys. Rev. B **64**, 224406 (2001).

[8] M. Mézard, G. Parisi, N. Sourlas, G. Toulouse, and M. A. Virasoro, J. Phys. **45**, 843 (1984).

[9] S. Franz and F. Ricci-Tersenghi, Phys. Rev. E **61**, 1121 (2000).

[10] S. Ciliberti and E. Marinari, cond-mat/0304273.

[11] G. Hed, E. Domany, and A. P. Young, to be published.

[12] M. Mézard, private communication.

[13] G. Hed, A. K. Hartmann, D. Stauffer, and E. Domany, Phys. Rev. Lett. **86**, 3148 (2001).

[14] In Ref. 7 we used Ward's clustering method, which tends to ignore pure states with small statistical weight. The present scheme is more suitable for our data, but the results of the analysis are similar for both schemes.

[15] A. K. Jain and R. C. Dubes, *Algorithms for Clustering Data* (Prentice–Hall, Englewood Cliffs, 1988).

[16] F. Guerra, Int. J. Mod. Phys. **10**, 1675 (1996).

[17] M. Aizenman and P. Contucci, J. Stat. Phys. **92**, 576 (1998).

[18] G. Parisi and F. Ricci-Tersenghi, J. Phys. A **33**, 113 (2000).

[19] This must hold if $P_J(q)$ is a finite sum of δ-functions (G. Parisi, private communication).

[20] E. Marinari, G. Parisi, F. Ricci-Tersenghi, J. Ruiz-Lorenzo, and F. Zuliani, J. Stat. Phys. **98**, 973 (2000).

Tables

3dISG			SK			Naive SK	
N	$\overline{K}$	$P(K=1)$	N	$\overline{K}$	$P(K=1)$	$\overline{K}$	$P(K=1)$
4^3	0.357(12)	0.617(16)	32	0.331(9)	0.350(16)	0.316(6)	0.759(7)
5^3	0.576(12)	0.233(13)	128	0.346(8)	0.037(5)	0.405(4)	0.365(7)
6^3	0.548(10)	0.144(9)	256	0.294(7)	0.005(1)	0.423(3)	0.127(4)
8^3	0.502(12)	0.044(5)	512	0.236(6)	$5(3)\ \times 10^{-4}$	0.395(2)	0.015(1)
			1024	0.182(5)	$2(1)\ \times 10^{-6}$	0.345(3)	$1.8(2)\ \times 10^{-4}$

TABLE I: The values of $\overline{K}$ as a function of N, for both the SK and 3dISG. See text for definitions.

3dISG			SK		
N	$[s_{\mathcal{C}_1\mathcal{C}_2}]_{\rm av}$	$[S_{\mathcal{C}_1\mathcal{C}_2}]_{\rm av}$	N	$[s_{\mathcal{C}_1\mathcal{C}_2}]_{\rm av}$	$[S_{\mathcal{C}_1\mathcal{C}_2}]_{\rm av}$
4^3	0.050(2)	0.135(7)	32	0.098(3)	0.338(29)
5^3	0.045(2)	0.123(6)	128	0.064(2)	0.196(12)
6^3	0.043(2)	0.133(10)	256	0.054(2)	0.170(10)
8^3	0.042(2)	0.136(9)	512	0.043(1)	0.142(10)
			1024	0.034(1)	0.115(10)

TABLE II: The standard deviation $s_{\mathcal{C}_1\mathcal{C}_2}$ and the normalized standard deviation $S_{\mathcal{C}_1\mathcal{C}_2}$ of the elements of $q_{\mathcal{C}_1\mathcal{C}_2}$ (see text), averaged over realizations of the disorder $\{J\}$, for 3dISG and SK systems of different sizes.

Figures

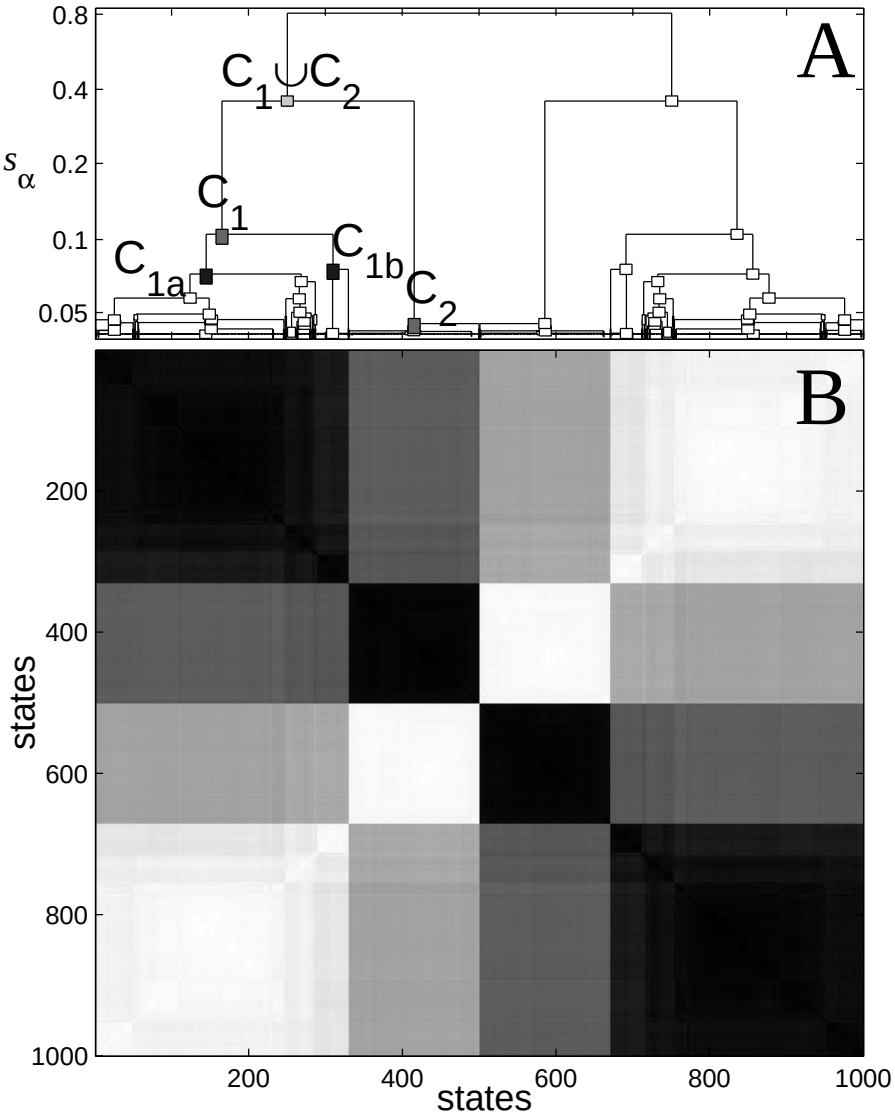

FIG. 1: (A) Clustering produces the dendrogram of state clusters, for the equilibrium ensemble of 1000 states, obtained by simulation of one realization of the SK model for 1024 spins, at $T = 0.2$. The vertical position of each cluster α is its score s_α. Logarithmic scale is used for the vertical axis; only clusters with $s_\alpha > 0.04$ are shown. Significant clusters, identified by a long branch above them, have high values of v_α; these clusters reflect presence of dense regions in the underlying Boltzmann distribution. (B) The distance matrix $d_{\mu\nu}$ of the microstates, that were reordered according to their positions, as the leaves of the dendrogram, on the horizontal axis of (A). Darker colors indicate smaller distances.

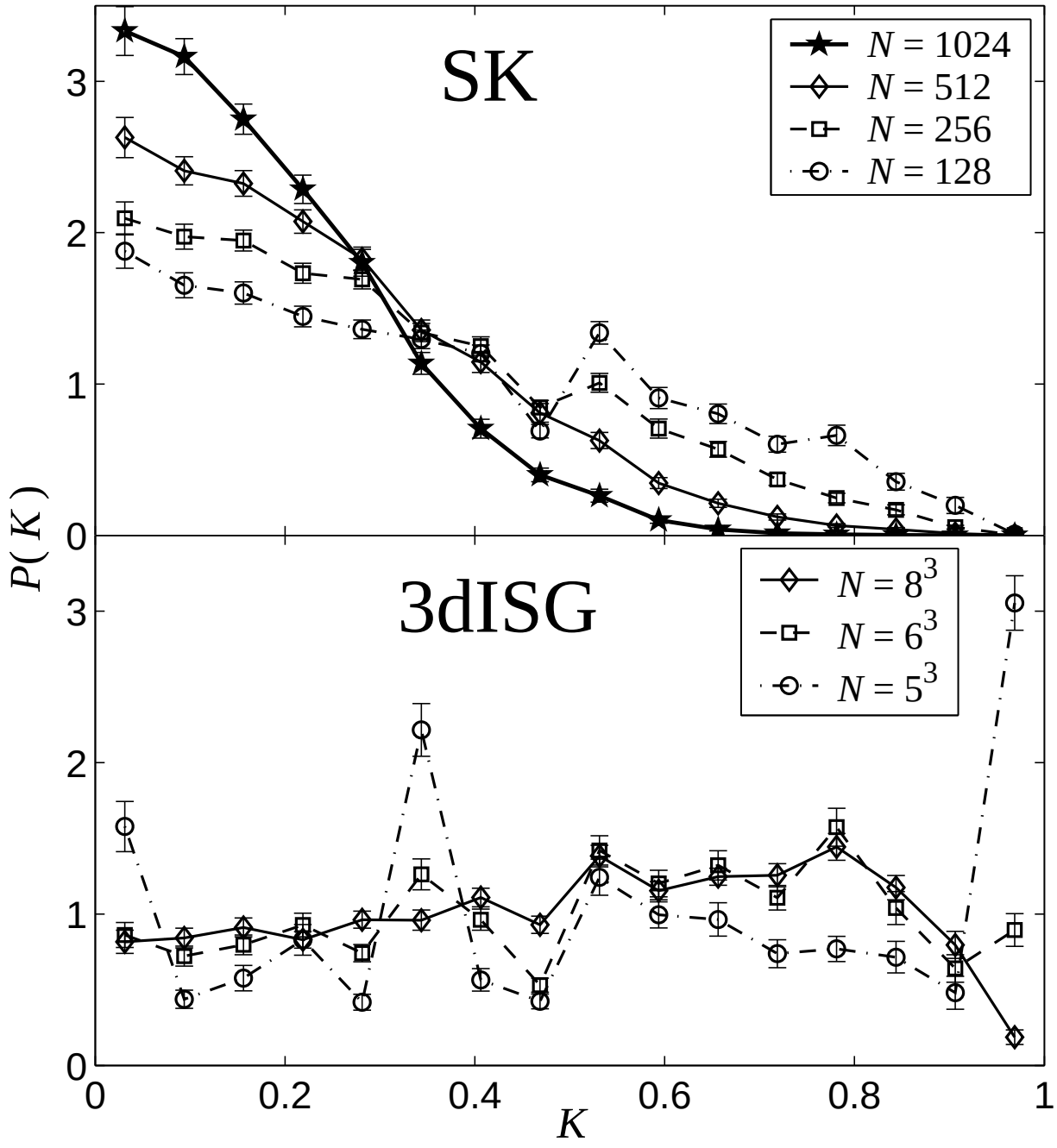

FIG. 2: The distributions $P(K)$ (see text), calculated for 3dISG and SK systems for various sizes N.

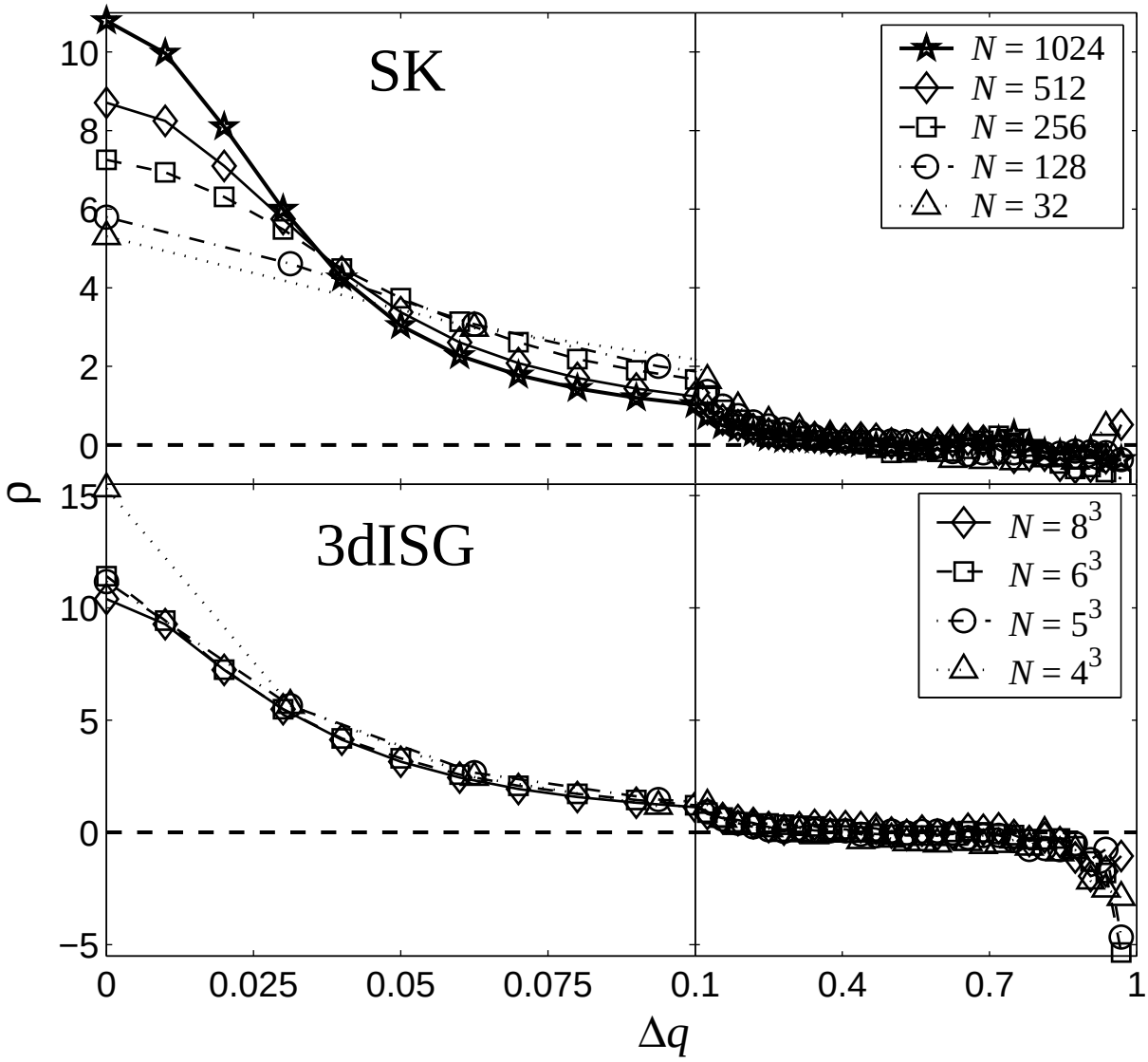

FIG. 3: The function $\rho(\Delta q)$ for SK and 3dISG systems. The error bars are smaller than the symbols.

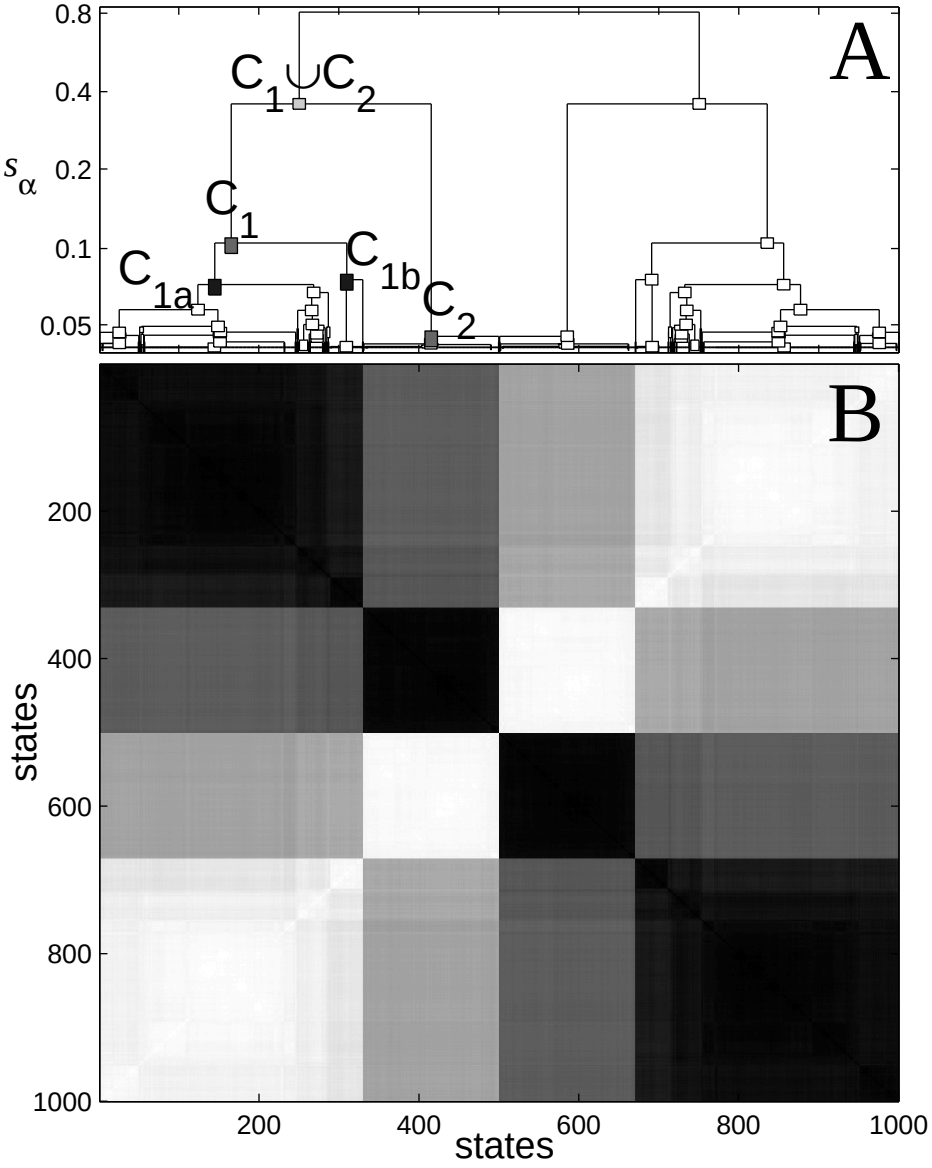
A
B
s_α
0.8
0.4
0.2
0.1
0.05
$C_1 \cup C_2$
C_1
C_{1a}
C_{1b}
C_2
200
400
600
800
1000
states
states

Figure 1

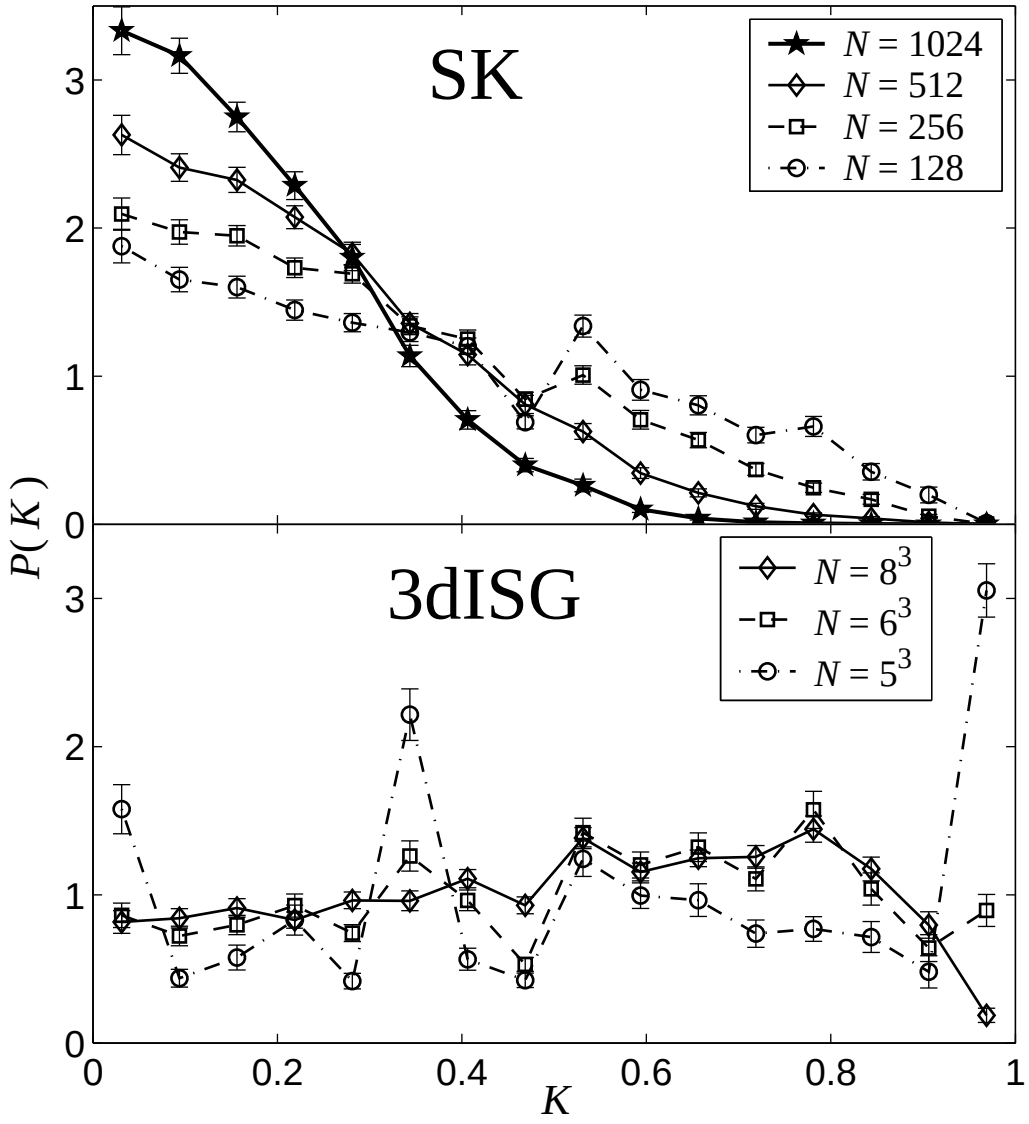

Figure 2

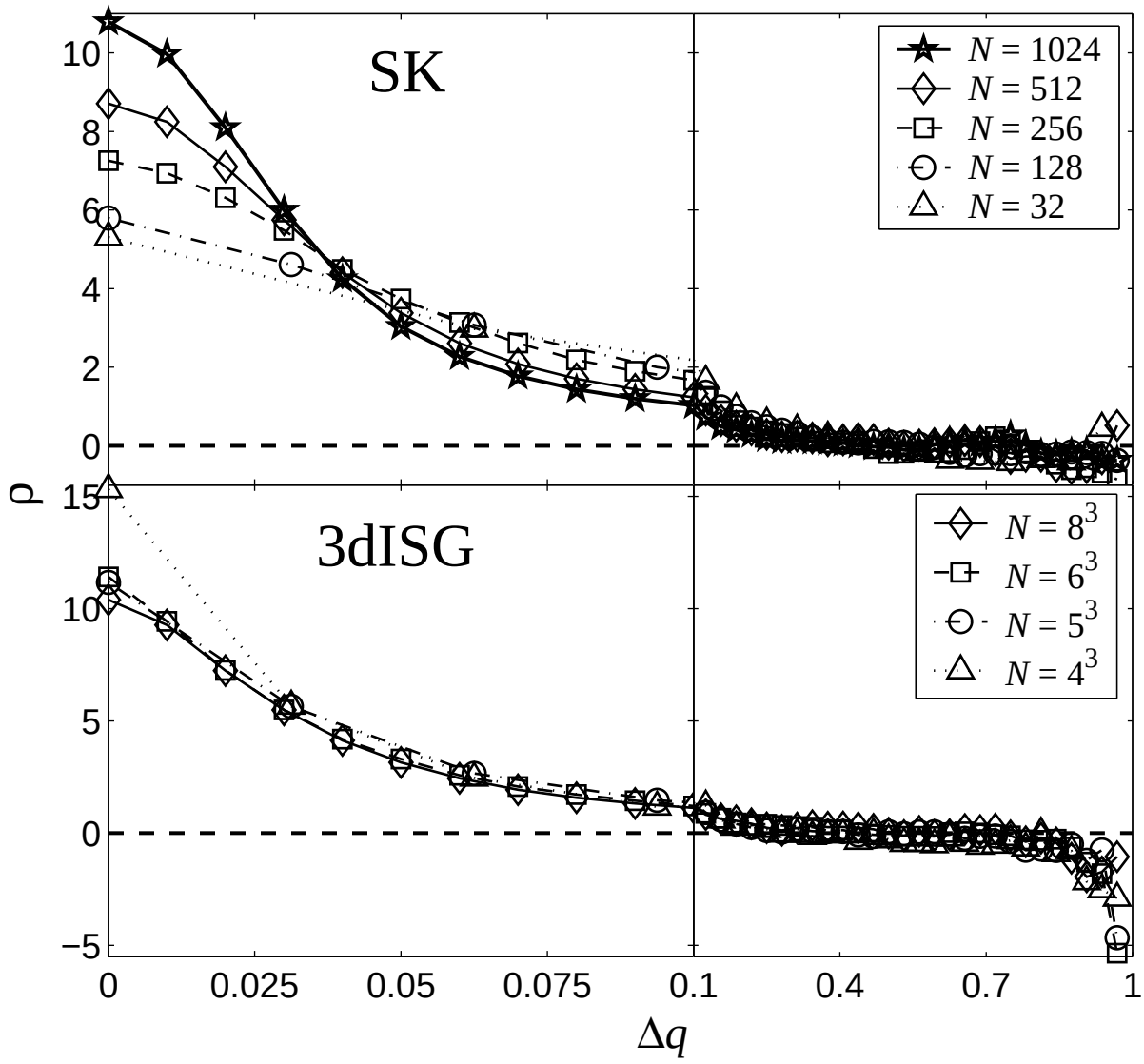
SK
3dISG
$N = 1024$
$N = 512$
$N = 256$
$N = 128$
$N = 32$
$N = 8^3$
$N = 6^3$
$N = 5^3$
$N = 4^3$
P
Δq
10
8
6
4
2
0
15
10
5
0
−5
0
0.025
0.05
0.075
0.1
0.4
0.7
1

Figure 3